Shear Piezoelectricity of Poly(L-lactide) Films Manufactured by Extrusion–Orientation: An Insight on Process–Structure–Property Relationships

Mohamed Aymen Ben Achour, Sophie Barrau, Jean-François Tahon, Mohamed Rguiti, Christian Courtois, Birgit Stubbe, Jean-Marie Raquez, Marie-France Lacrampe, Cédric Samuel

Shear Piezoelectricity of Poly(L-Lactide) Films Manufactured by Extrusion – Orientation: An Insight on Process – Structure – Properties Relationships

Mohamed Aymen Ben Achour [1], Sophie Barrau [2], Jean-François Tahon [2], Mohamed Rguiti [1], Christian Courtois [1], Birgit Stubbe [3], Jean-Marie Raquez [4], Marie-France Lacrampe [5], Cédric Samuel [5*]

[1] Univ. Polytechnique Hauts-de-France, INSA Hauts-de-France, CERAMATHS – Laboratoire de Matériaux Céramiques et de Mathématiques, F-59313 Valenciennes, France

[2] Univ. Lille, CNRS, INRAE, Centrale Lille, UMR 8207 – UMET – Unité Matériaux et Transformations, F-59000 Lille, France

[3] Centexbel, Technologiepark 70, B-9052 Zwijnaarde, Belgium

[4] University of Mons (UMons), Laboratory of Polymeric and Composite Materials (LPCM), Center of Innovation and Research in Materials and Polymers (CIRMAP), Place du Parc 20, B-7000 Mons, Belgium

[5] IMT Nord Europe, Institut Mines-Télécom, Univ. Lille, Centre for Materials and Processes, F-59000 Lille, France

Corresponding author: Dr. Samuel Cédric – samuel.cedric@imt-nord-europe.fr

Abstract: Shear piezoelectric properties of uniaxially-stretched poly(L-Lactide) (US-PLA) films manufactured by an industrially-relevant technique (*i.e.* extrusion – orientation without poling) are investigated and specific insight on the process – structure – properties relationships is provided. Two commercially available PLA grades with D-isomer content between 2 – 4 % are selected. The shear piezoelectric coefficient d_{14} of US-PLA films tends to increase with the draw ratio applied during the orientation stage and a maximal d_{14} of 5.9 pC/N is reported. However, a dramatic degradation of piezoelectric properties could be observed at elevated draw ratio, in particular for PLA grades with low D-isomer content. Structures induced by the orientation stage are subsequently explored and relations with shear piezoelectric properties are discussed. The mesophase is detected by DSC / WAXS up to draw ratio 4 after being replaced by strain-induced crystallization at higher draw ratios. The orientation state of the amorphous phase, mesophase and α'-crystals is assessed by 2D-WAXS and polarized FTIR. Piezoelectric properties obtained at a moderate draw ratio are supported by the amount/orientation of each phase (partly-oriented amorphous phase and fully-oriented mesophase/α'-crystal phase). A model is proposed to evaluate the contribution of each phase. However, other structural parameters deserve careful attention at elevated draw ratios, in particular mechanical damage and formation of voids/cavities. 2D-SAXS analysis coupled with complementary characterizations indicates that the amount of voids/cavities controls the deterioration of shear piezoelectric performances at high draw ratios. This phenomenon is critical for highly crystalline PLA grades. A final discussion is dedicated to the quality of α'-crystals formed by current orientation conditions, a factor that could also limit the d_{14} coefficient of US-PLA films. This work consequently demonstrates that environmental-friendly piezoelectric films could be manufactured by a straightforward process of the plastic industry and opens up several scientific/technological perspectives for their future implementation into practical applications.

Keywords: Poly(L-Lactide), Extrusion, Orientation, Piezoelectricity, Process-structure-properties relationships.

1. Introduction

Electroactive polymers, particularly piezoelectric polymers, represent strategic technological bricks for future flexible electronic systems. Compared to traditional piezoelectric ceramics, piezoelectric polymers display multiple advantages such as high flexibility, high ductility/toughness, and ease-of-manufacturing into complex shapes. More importantly, piezoelectric polymers clearly avoid any use of hazardous and critical raw materials. Many research activities were focused on piezoelectric fluoropolymers such as poly(vinylidene fluoride) (PVDF) and related copolymers that display the highest piezoelectric performances among all thermoplastic polymers ($-d_{33} \approx 30 - 40$ pC/N and $d_{31} \approx 20 - 25$ pC/N)[1–9]. Numerous smart applications were demonstrated from mechanical sensors (stress, strain, vibration, and impact sensors) to acoustic/ultra-sound transducers and high-precision actuators[1–3,10–18]. Vibrational energy harvesters based on piezoelectric polymers are also envisioned for the development of self-powered electronic devices. However, the main technical limitation of fluoropolymers is linked to the poling post-treatment requiring extreme electrical fields (higher than 1000 – 1500 kV/cm), a complex step to handle at the laboratory/industrial scale. Fluoropolymer costs and health – environmental aspects related to fluoropolymer synthesis/processing also represent some important issues. Significant piezoelectric properties were attested for optically-active polymers without any high-voltage poling. Poly(L-Lactide) (PLA), a well-known thermoplastic polymer with a high industrial maturity and high environmental attributes, could represent an ideal candidate for piezoelectric application and deserves a careful attention.

The piezoelectricity of optically-active polymers is radically different from the piezoelectricity of PVDF. Polar β-PVDF crystals are piezo-ferroelectric (according to their orthorhombic crystal structure and *mm2* space group) and the application of strong electric fields is fundamental for dipole organization into a preferential direction. A macroscopic polarization and piezoelectric properties are subsequently obtained according to a classical piezoelectric tensor (**Figure 1**).

Optically-active polymers such as PLA display peculiar shear piezoelectricity properties without high-voltage poling. A uniaxial orientation state is only required to induce a specific tensor linked to a D_∞ symmetry (**Figure 1**). Note that PLA is non-ferroelectric and a macroscopic polarization is only obtained with the application of shear stresses/strains. Piezoelectric coefficients d_{14} in the range 10 – 20 pC/N are reported for uniaxially-stretched poly(L-Lactide) (US-PLA) films[1,10,11,19–36] and, due to a low dielectric permittivity, shear piezoelectric voltage coefficients g_{14} up to 350 – 800 mV.m/N are attested[21,24,35]. These piezoelectric performances are competitive with PVDF ($g_{31} \approx 200$ mV.m/N, $-g_{33} \approx 500$ mV.m/N)[3,4,9,21,37] and multiple smart applications were demonstrated for piezoelectric PLA films/fibers (osteo-regeneration, biomedical catheters/tweezers, rotatory actuators, touch sensors, body movement sensors, etc)[20,27,29,31–34]. Efficient piezoelectric energy harvesters based on a piezoelectric PLA layer were also recently developed[25,26] and, based on simple electromechanical models, our group recently demonstrate competitive energy harvesting performances of US-PLA films compared to PVDF films[38]. PLA consequently represent an ideal candidate for a next-generation of piezoelectric materials combining high technical performances, high environmental attributes, low material costs and aptitude to large-scale industrial processing.

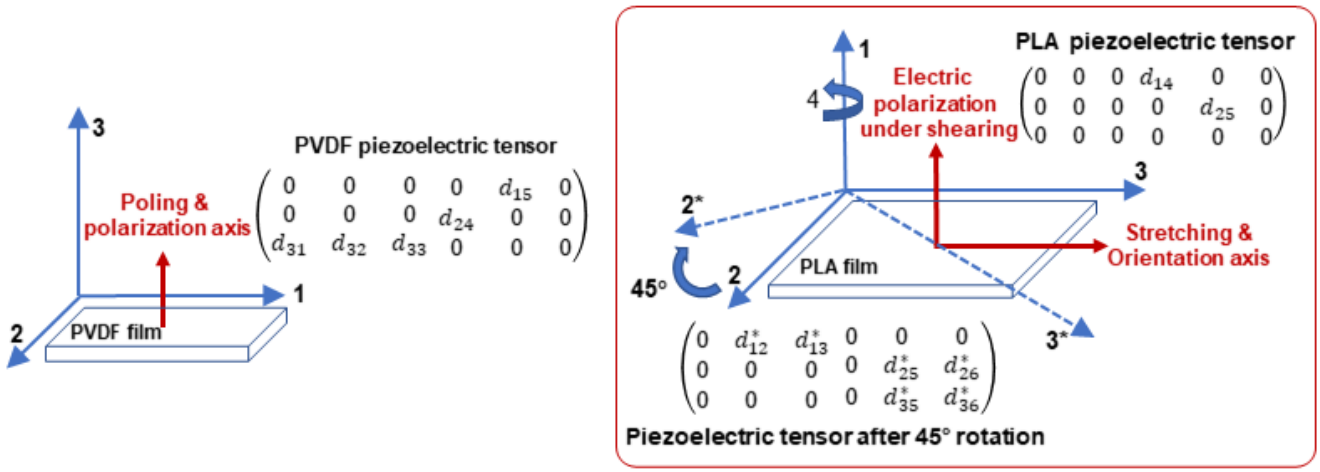

***Figure 1**. Coordinate systems used to describe the piezoelectricity of poled PVDF films and US-PLA films with respective piezoelectric tensors. Modified piezoelectric tensor for 45°-cut US-PLA films (detailed mathematical operations regarding the matrix transformation by a clockwise 45°-rotation around the axis 1 could be found elsewhere[39], definition of the direction cosine matrix and stress transformation matrices). (Figure partly reproduced from). Reprinted (Adapted or Reprinted in part) with permission from Ben Achour M.A. et al.[40] Copyright 2022 John Wiley & Sons.*

An important issue relates to the current knowledge about piezoelectric performances of PLA and the precise relationships to macromolecular/structural parameters. This aspect is of high scientific importance and could enable faster developments of practical applications. Fukada E. early reported shear piezoelectric performances of US-PLA films (draw ratio up to 6, stretching temperature 80°C, annealing temperature 110°C) with maximal d_{14} close to 10 – 13 pC/N[1,20,21]. These piezoelectric performances are confirmed in many studies on US-PLA films. Fukada E. suspected that crystalline regions play a key role and the amount of PLA crystals (*i.e.* crystallinity index X_c) was considered in a two-phase model for experimental dielectric/piezoelectric relaxations (piezoelectric PLA crystals embedded into a non-piezoelectric amorphous matrix). The importance of X_c on shear piezoelectric properties of US-PLA was highlighted and outstanding shear piezoelectric coefficients of PLA crystals $d_{14}^{cystals}$ close to 30 pC/N were concluded. The degree of orientation of PLA crystals (F_c) is also of prime importance and this aspect was investigated by Lovell C.S. et al.[22]. For moderate degree of orientation (F_c lower than 0.35), the piezoelectric coefficient d_{14} was found proportional to the product $X_c.F_c$, as a classical result for many biobased piezoelectric materials, and the exceptional shear piezoelectric coefficients of PLA crystals was confirmed ($d_{14}^{cystals}$ close to 28.5 pC/N). However, the crystallinity index X_c and the degree of orientation F_c cannot explain many experimental results on shear piezoelectric properties of US-PLA films, in particular at elevated degree of orientation (or elevated draw ratio). Fukada E. found an optimum draw ratio close to 4 – 5 and a saturation/degradation of piezoelectric performances is observed at higher draw ratio[20]. Such effects are also attested by Mat Zin S.H. et al.[23]. Actually, at elevated X_c and/or F_c, the shear piezoelectric coefficient d_{14} is no longer proportional to the product $X_c.F_c$ and a saturation of piezoelectric performances is attested. No detailed structural data are reported but shear piezoelectric performances of PLA are probably controlled by other structural parameters in these elevated X_c and/or F_c ranges.

Advanced data about shear piezoelectric performances of US-PLA films were reported by Tajitsu Y. and al. using various PLA grades (different M_w and optical purity), various additives

(methacrylic additives or stereocomplexes) and various orientation techniques/conditions (uniaxial stretching – annealing, solid-state extrusion, supercritical CO_2 post-treatments)[27–36]. From these intensive research activities, outstanding shear piezoelectric performances up to 16 – 21 pC/N were obtained and several conclusions were extracted. Tajitsu Y. and al. proved that the use high-M_w and optically-pure PLA (optical purities close to 99.99 %, melting temperatures in the range 185 – 190°C) enhanced final piezoelectric properties of US-PLA films[31,32]. Specific methacrylic additives such as PMMA-*b*-PBA-*b*-PMMA also improve the piezoelectric performances of US-PLA films[30,31]. Tajitsu Y. and al. finally proved that orientation conditions (draw ratio up to 12, stretching – annealing temperatures up to 160°C) and post-treatments by supercritical CO_2 are fundamental to provide the highest piezoelectric performances for PLA. No correlations between d_{14} and $X_c - F_c$ are attested and results were mainly interpreted in terms of *"homogenous high-order structures"* that could be related to the quality of oriented crystalline/amorphous phases. In-depth structural analyses seem of major importance to get deeper information about these structures with links between macromolecular/processing parameters and final piezoelectric performances of PLA.

Interestingly, the structural ordering durinthe g stretching processes of PLA in the rubbery state (*i.e.* above glass transition temperature) represents an intensive research theme covered by numerous authors[41–52]. The structural ordering of PLA during uniaxial stretching is amazingly complex and PLA could undergo various phenomenon from amorphous phase orientation to the apparition of mesomorphic phases (or mesophase) and/or strain-induced crystalline phases. The strain-induced crystalline phases could be also broken or transformed into new crystal phases according to α'-to-α or α-to-β crystal transitions. Formation of micro-voids due to cavitation phenomenon is also commonly observed. The amount of each phase, their respective degree of orientation and the intensity of damage mechanisms depends on many macromolecular/stretching parameters (M_w, optical purity, draw ratio, strain rate, stretching temperature, initial structures, etc). Advanced experimental techniques such as differential scanning calorimetry (DSC), wide-angle/small-angle X-ray scattering (WAXS / SAXS) and polarized infra-red spectroscopy (FTIR)

are used to investigate the structural ordering of PLA during uniaxial stretching. The above studies are usually performed for improving engineering properties of PLA such as (thermo)mechanical and optical/barrier properties and, to the best of our knowledge, no link with shear piezoelectric performances of US-PLA films have been performed. A correlation could be envisioned with *"homogenous high-order structures"* mentioned by Tajitsu Y. and al. and, in this respect, in-depth qualitative/quantitative structural analyses are mandatory for a better scientific knowledge on shear piezoelectric properties of PLA.

Such scientific knowledge is also fundamental for the optimization of processing techniques/conditions and initial formulations in order to develop high-performances shear piezoelectric films. Actually, the processing of PLA into US-PLA could be easily handled at the industrial scale by standard processing technologies of the plastic/textile industry. Incorporation of additives into PLA could be done by twin-screw extrusion and its subsequent transformation into US-PLA films only requires single-screw extruders with machine-direction orientation stations (MDO)[53,54]. Intense uniaxial elongational flows are applied by MDO and this process continuously manufacture highly-oriented films with a good control over orientation conditions (draw ratio, strain rate, stretching temperature, annealing temperature in stretched state, etc). MDO consequently seems to be an ideal processing technique for a large-scale production of US-PLA films with enhanced shear piezoelectric properties but, to the best of our knowledge, extrusion processing coupled to MDO has never been investigated for this purpose.

In this scientific and technical context, our study is dedicated to the manufacturing of shear piezoelectric PLA films by an industrially-relevant technique without high-voltage poling (*i.e.* extrusion – orientation or extrusion – MDO) and a specific insight on process – structure – properties relationships is reported. For these purposes, two commercially-available and high-molecular weight PLA grades suitable for extrusion processing and displaying different optical purities are selected (PLA 4032D and PLA 2003D from NatureWorks®). In a first part, shear piezoelectric performances of as-produced US-PLA films are evaluated with respect to the applied

draw ratio during the orientation step. Different trends are clearly detected depending on the PLA grades. Subsequent parts are dedicated to structural analyses of as-produced US-PLA films by multiple techniques (including DSC, 2D-WAXS, polarized FTIR, 2D-SAXS and DMA) to highlight and discuss about key structural features controlling final piezoelectric performances.

2. Experimental section

2.1. Materials and processing

Poly(L-lactide) (PLA) pellets were supplied by NatureWorks®. Two PLA grades with similar weight-average molecular weights (M_w), similar melt flow rates (MFR) and different optical purities (D-isomer content) were used, namely PLA 2003D (M_w 180,000 g/mol, MFR 6 g / 10 min, D-isomer content 4.3 %, T_m 145 – 160°C, T_g 55 – 60°C) and PLA 4032D (M_w 185,000 g/mol, MFR 7 g / 10 min, D-isomer content 1.4 – 2.0 %, T_m 155 – 170°C, T_g 55 – 60°C) (data from manufacturer and literature)[55,56].

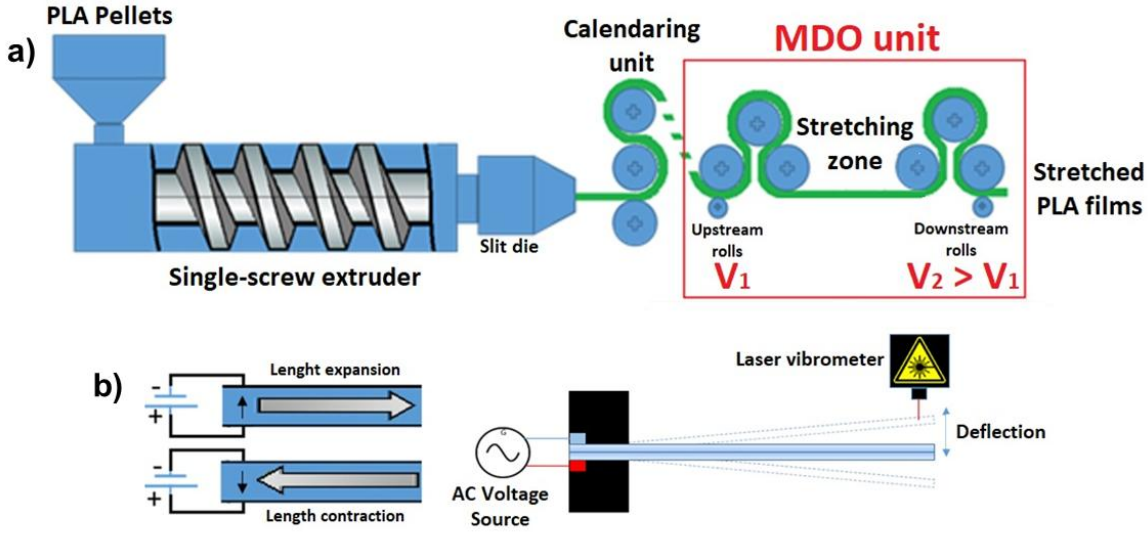

***Figure 2**: (a) Schematic representation of the extrusion – orientation (extrusion – MDO) processing technique to manufacture US-PLA films with shear piezoelectric properties without poling. The process used in this study is performed in a discontinuous manner (PLA films extrusion in a first part film followed by converting into US-PLA films by MDO in a second part). (b) Schematic representation of the length expansion - contraction of metallized piezoelectric strips with the application of an electric field. Measurement technique for d_{13}* coefficients by applying a sinusoidal voltage on a bimorph piezoelectric cantilever and measuring of the beam deflection of*

the free end by a laser vibrometer. Reprinted (Adapted or Reprinted in part) with permission from Ben Achour M.A. et al.[40] Copyright 2022 John Wiley & Sons.

The production process of uniaxially-stretched PLA films (US-PLA) from PLA pellets is depicted in **Figure 2a**. PLA films were first produced by extrusion-calendaring with a single-screw extruder (Haake Rheocord System 40, L/D ratio ≈ 16, temperature profile 180 – 195 – 195 – 190°C from the hopper to the die, screw speed 60 rpm) equipped with a calendaring unit. A specific slit die for film extrusion (width 150 mm, thickness 800 µm) was used and extrudates were cold-calendared to obtain 300 µm-thick films with a width close to 9 cm. PLA films were post-treated by a machine-direction orientation process (MDO, Teachline MDO-AT, Collin) to obtain US-PLA films. The uniaxial stretching is performed at 60°C (just above the glass transition temperature of PLA) and apparent draw ratio from 2 to 6 are targeted (up to film rupture). The apparent draw ratio is calculated by the ratio between the linear speed of downstream rolls and upstream rolls (linear speed of the upstream roll 1 m/min, varying linear speed of the downstream roll 2 – 6 m /min). Final thicknesses of US-PLA films are reported in **Table 1** (evaluated by a mechanical comparator, precision +/- 1 µm). It can be mentioned that the proposed extrusion – MDO process is performed in a discontinuous manner because calendaring and MDO units are decoupled. This configuration insures flexibility, conveniency and good film quality at our laboratory scale. However, a continuous process could be easily envisioned at the industrial scale using dedicated calendaring – MDO units with a direct coupling[53,54].

2.2. Characterizations

2.2.1. Measurement of shear piezoelectric coefficients

The shear piezoelectric properties of as-produced US-PLA films were evaluated by a bimorph cantilever technique previously reported by our group[40]. This method can measure the shear piezoelectric coefficient d_{14} of current US-PLA films with a good accuracy and a precision close to 10 %. Both sides of US-PLA films were first metallized by spray-coating with a silver paint supplied by CDS Electronique® (grade L-200N) and metallized strips were cut at 45° from the

stretching direction (corresponding to a length-expansion 13*-mode according to the modified piezoelectric tensor depicted in **Figure 1**). Bimorph cantilevers were assembled using two strips glued together with Loctite 435 according to **Figure 2b**. In this configuration, an electric field induces a bending deformation of the clamped beam due to a simultaneous length-expansion/contraction of the opposite strips. By measuring the beam deflection at various voltages, the piezoelectric coefficient d_{13}* and d_{14} can be readily determined using **Equation 1-2**.

$$d_f \approx \frac{3}{2}\frac{l^2}{t^2} d_{31} V \quad (1)$$

$$d_{13}^* = \frac{1}{2} d_{14} \quad (2)$$

with d_f the beam deflection at the free end (m), l the beam length (m), t the total thickness of the beam, d_{13}* the piezoelectric coefficient (m/V), d_{14} the shear piezoelectric coefficient (m/V) and V the applied voltage (V).

Bimorph cantilevers were excited with an AC voltage source (Radiant Technologies, model Precision 10 kV HVI-SC) according to **Figure 2b**. Sinusoidal AC voltages with amplitudes in range 100 – 1500 V and frequencies in the range 3 – 7 Hz were used. The beam deflection is measured using a portable digital vibrometer (Polytec, model PVD1000). The distance between the fixed end and the laser spot was set to 35 mm (approaching the free end of the beam as much as possible). Between six and eight bimorph cantilevers were tested for each material.

2.2.2. Differential scanning calorimetry (DSC)

The thermal properties of as-produced US-PLA films were obtained by differential scanning calorimetry (DSC) using a DSC Q20 apparatus (TA Instruments) calibrated with high purity indium. Samples of approximately 10 mg were put in aluminum pans and analyzed in the temperature range 10 – 220°C at a heating rate of 10°C.min^{-1} under nitrogen flow. The degree of crystallinity X_c of as-produced US-PLA films was estimated from the first heating scan by using **Equation 3**.

$$X_c = \frac{\left(\Delta H_{m,PLA} - \Delta H_{c,PLA}\right)}{\Delta H_{m,PLA}^0} \quad (3)$$

with $\Delta H_{m,PLA}$ the melting enthalpy (J/g), $\Delta H_{c,PLA}$ the cold crystallization enthalpy (J/g) and $\Delta H^0_{m,PLA}$ the melting enthalpy of 100 % crystalline PLA (93 J/g).

2.2.3. X-Ray analysis

Wide angle X-ray scattering (WAXS) and small-angle X-ray scattering (SAXS) experiments were carried out on a Xeuss 2.0 (Xenocs) operating under vacuum with a GeniX3D microsource (CuK_α radiation, λ = 1.54 Å at 0.6 mA – 50 kV) and a 2D Pilatus 3 R 200 K detector. Analyses of as-produced US-PLA films were performed in transmission mode. The two-dimensional WAXS patterns (2D-WAXS) were acquired with a sample-to-detector distance of 160 mm while two-dimensional SAXS patterns (2D-SAXS) were acquired with a sample-to-detector distance of 2300 mm. From the 2D patterns, WAXS and SAXS scattered intensities were integrated and plotted against the scattering angle 2θ and the scattering vector q respectively. The orientation is calculated using the Herman's orientation function (f) from the integrated intensity plotted versus the azimuthal angle (ϕ) from 0° to 180° at a defined 2θ angle (**Equation 4-5**). Note that an orientation function f of 1 indicates for perfect parallel orientation and an orientation function f of 0 indicates no orientation.

$$f = \frac{3\,\langle cos^2\,\theta\rangle - 1}{2} \qquad (4)$$

$$\langle cos^2\,\theta\rangle = \frac{\int_0^{\pi/2} I(\phi).sin\phi.cos^2\phi.d\phi}{\int_0^{\pi/2} I(\phi).sin\phi.d\phi} \qquad (5)$$

with θ the angle between the normal of a given (hkl) crystal plane and the stretching direction (θ = 0 corresponds to the stretching direction).

2.2.4. Polarized FTIR

As-produced US-PLA films were analyzed by Fourier-Transform InfraRed spectroscopy (FTIR) and experiments were carried out on a Nicolet iS-20 FTIR spectrometer (ThermoFisher, KBr beamsplitter, DTGS KBr detector) equipped with a ZnSe polarizer (ThermoScientific). Analyses were performed in transmission mode. Spectra were acquired (i) without polarizer, (ii) with a light polarized at 0° regarding the stretching direction and (iii) with a light polarized at 90° regarding the

stretching direction. Spectra were collected after 64 scans at a resolution of 2 cm^{-1} in the range 600 – 4000 cm^{-1}. Backgrounds were also collected before each analyses and spectra were displayed with baseline correction and without smoothing treatment.

2.2.5. Shear modulus and density measurements

The shear modulus of US-PLA films was evaluated by a Dynamic Mechanical Analyzer (DMA, Metravib +150) equipped with a 2-gap film shearing device (total gap length 10 mm, film width 10 – 15 mm, shear applied perpendicular to the stretching direction). Measurements were performed at room temperature with a shearing frequency of 10 Hz and a dynamic displacement comprised between 5 – 10 µm. For density measurements, US-PLA films were cut into rectangular specimens with precise dimensions (approx. to 2 x 4 cm) and their weight were measured with Mettler Toledo XA105 precision balance (resolution 0.01 mg).

3. Results and discussions

3.1. Shear piezoelectric properties of US-PLA films as a function of the draw ratio

US-PLA films were produced by extrusion – MDO and draw ratio up to 6 were easily reached during the MDO stage (performed at 60°C in a continuous manner from extruded films). Dimensions of US-PLA films after the MDO stage are tabulated into **Table 1** and a reduction of the film widths/thicknesses is attested with the applied draw ratio. It can be here noticed that higher draw ratios (> 6) induce PLA film breaking during the MDO stage and that higher draw temperatures (> 65°C) induce PLA film sticking to metal rolls with large process instabilities. This MDO stage performed in the rubbery state of PLA is believed to produce US-PLA films with a high orientation state and these films are expected to display significant shear piezoelectric properties. Two industrially-available PLA grades suitable for extrusion were used and these two grades only differ by their optical purity (1.4 – 2 % *vs.* 4.2 % of D-isomer for PLA 4032D and PLA 2003D respectively). Such differences in terms of optical purity could modify both the structuration of US-PLA films during the MDO stage and their subsequent shear piezoelectric properties.

Figure 3 displays the evolution of the shear piezoelectric coefficient d_{14} as a function of the draw ratio for US-PLA films made from the two PLA grades. Precise values with standard deviations are tabulated in **Table 1**. The MDO stage is clearly fundamental to impart significant shear piezoelectric properties to PLA films. Actually, even for small draw ratio close to 2, shear piezoelectric coefficients d_{14} in the range 0.5 – 1 pC/N are attested for US-PLA films. The piezoelectric activity of US-PLA increases with draw ratio and, at intermediate draw ratio between 3 – 4, a higher shear piezoelectric coefficient is obtained for PLA 4032D (low D-content) compared to PLA 2003D (high D-content). For instance, US-PLA films made from PLA 4032D reached d_{14} values close to 5.2 pC/N for a draw ratio of 4 whereas US-PLA films made from PLA 2003D only attained d_{14} values close to 3.0 pC/N. However, for extreme draw ratio up to 5 – 6, a drastically different situation is observed with a dramatic deterioration of shear piezoelectric properties only observed for US-PLA films made from PLA 4032D. On the contrary, the shear piezoelectric properties of US-PLA films made from PLA 2003D continue to increase up to a maximal shear piezoelectric coefficient d_{14} close to 5.9 pC/N. This d_{14} value represent the best value obtained in this study. As a first conclusion, the optical purity of PLA and the applied draw ratio during the MDO stage both represent important material/processing parameters that partly control final shear piezoelectric properties of US-PLA films. However, structural features obtained during the MDO stage are suspected to play a role and these aspects are covered in the next sections to get a better insight on structure – shear piezoelectric properties relationships and their links to material/processing parameters.

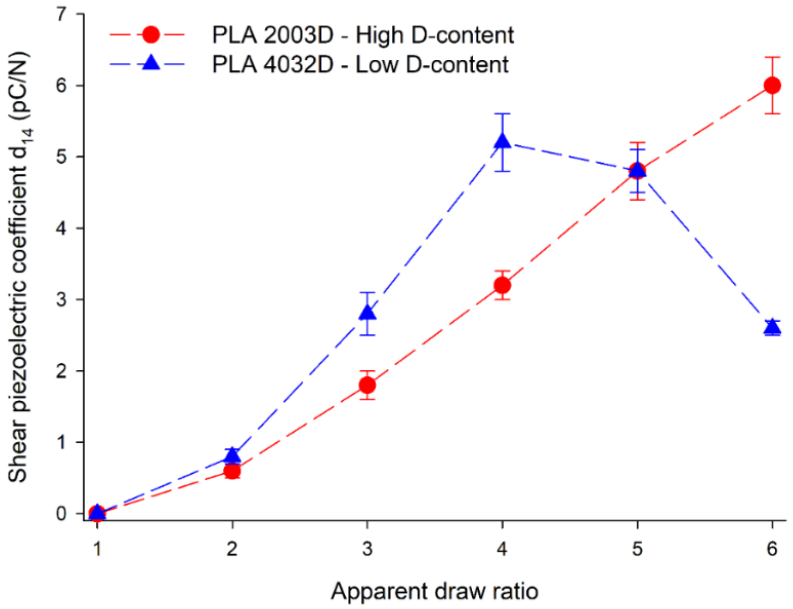

Figure 3*. Evolution of the shear piezoelectric coefficients with the applied draw ratio for US-PLA films obtained by extrusion – MDO. US-PLA films made from PLA 2003D (High D-content, red) and US-PLA films made from PLA 4032D (Low D-content, blue).*

Table 1*. Geometrical characteristics and quantitative values of the shear piezoelectric coefficients for US-PLA films produced by extrusion – MDO at various draw ratio.*

	Apparent draw ratio[1]	**Average thickness (µm)**[2]	**d_{14} (pm/V)**
PLA 2003D	1*	310	0
	2	260	0.7 (±0.1)
	3	210	1.8 (±0.1)
	4	150	3.0 (±0.2)
	5	130	4.8 (±0.3)
	6	110	5.9 (±0.6)
PLA 4032D	1*	300	0
	2	260	0.9 (±0.1)
	3	190	2.7 (±0.2)
	4	140	5.2 (±0.2)
	5	130	5.0 (±0.4)
	6	100	2.6 (±0.1)

[1] *Apparent draw ratio evaluated by the ratio between the linear speed of downstream rolls and upstream rolls (speed of the upstream roll 1 m/min, speed of the downstream roll 2 – 6 m /min).*

[2] *Standard deviation by approx. 10%.*[40]

** Original extruded film without uniaxial stretching by MDO step.*

3.2. Crystallinity and mesophase analysis of US-PLA films

The crystallinity of US-PLA films (degree of crystallinity X_c and type of crystals) represents the first structural parameters of interest and DSC analysis were first conducted. Thermograms of extruded PLA films before the MDO stage could be found in **Figure S1**. Typical heating scans of fully amorphous PLA films are obtained (well-defined glass transition in the range 55 – 60°C with endothermic enthalpy relaxations followed by exothermic cold crystallization and endothermic melting evens). The degree of crystallinity of extruded PLA films was found close to 0 % in accordance with many studies[57–59]. Thermograms of US-PLA films are also displayed in **Figure S1** and significant modifications are attested, in particular regarding the exothermic cold crystallization event. Actually, the cold crystallization temperature of US-PLA films (observed in the range 100 – 140°C) gradually decreases with the applied draw ratio during the MDO stage and this event totally vanishes for elevated draw ratio. These phenomena indicate the MDO stage enhanced the crystallization ability of PLA due to macromolecular orientation and that strain-induced crystals appear in US-PLA films obtained at elevated draw ratio. This later effect is also supported by the significant reduction of the heat capacity change at the glass transition for US-PLA films obtained at elevated draw ratio. Degrees of crystallinity of US-PLA films (evaluated by DSC using **Equation 3**) are tabulated in **Table 2**. For US-PLA films made from PLA 2003D (high D-content), strain-induced crystals appear in significative amounts for draw ratio 5 and the degree of crystallinity increases up to 28 % for draw ratio 6. For US-PLA films made from PLA 4032D (low D-content), the strain-induced crystallization appears in significative amount for draw ratio 4 and a higher degree of crystallinity up to 35 % is obtained for draw ratio 6.

Table 2*. Degree of crystallinity X_c (obtained by DSC and WAXS) and mesophase content (obtained by WAXS) of US-PLA films produced by extrusion – MDO at various draw ratio.*

	Draw ratio	**X_c (%) (DSC)**	**X_c (%) (WAXS)**	**Mesophase content (%) (WAXS)**	**$X_{meso\text{-}crystal}$ (%) (FTIR)**	**Peak position (cm^{-1}) (FTIR)**
PLA 2003D	1	0	0	2	2	917.9
	2	0	0	3 (±1)	4	918.3

	3	0	0	4 (±1)	6	918.5
	4	3	4	10 (±3)	13	918.8
	5	16	17	6 (±2)	27	920.1
	6	28	28	4 (±2)	35	920.4
PLA 4032D	1	0	0	3	2	917.8
	2	0	0	4 (±1)	5	918.3
	3	0	0	11 (±3)	9	918.5
	4	16	18	8 (±3)	33	920.3
	5	25	25	4 (±1)	35	920.5
	6	35	35	2 (±1)	44	920.4

WAXS analysis were subsequently performed to support the strain-induced crystallization of PLA films during the MDO stage at elevated draw ratio. WAXS intensity profiles of extruded PLA films before the MDO stage could be found in **Figure S2** and the amorphous nature of these films is confirmed with a typical broad halo centered on a 2θ value close to 15.5°. WAXS intensity profiles of US-PLA films are displayed in **Figure 4**. For US-PLA films made from PLA 2003D (high D-content), their amorphous nature is also confirmed at low draw ratio. Strain-induced crystals are clearly produced in significative amounts for draw ratios higher than 5 as attested by the appearance of a sharp peak located at a 2θ value of 16.3°. Similar phenomena are also observed for PLA 4032D but strain-induced crystals clearly appear at a lower draw ratio close to 4. In this respect, WAXS analysis confirmed previous conclusions made from DSC thermograms. Amorphous extruded PLA films are transformed into semi-crystalline US-PLA films during the MDO stage for draw ratio between 4 – 5 according to a strain-induced crystallization mechanism. The strain-induced crystallization was found more sensitive to draw ratio for US-PLA films made from PLA 4032D (low D-content) than US-PLA films made from PLA 2003D (high D-content). WAXS intensity profiles also confirmed the higher degree of crystallinity for US-PLA films made from PLA 4032D than US-PLA films made from PLA 2003D. Such differences between the two PLA grades are here

largely explained by their difference in terms of optical purity with an enhanced crystallization ability for PLA 4032D compared to PLA 2003D.

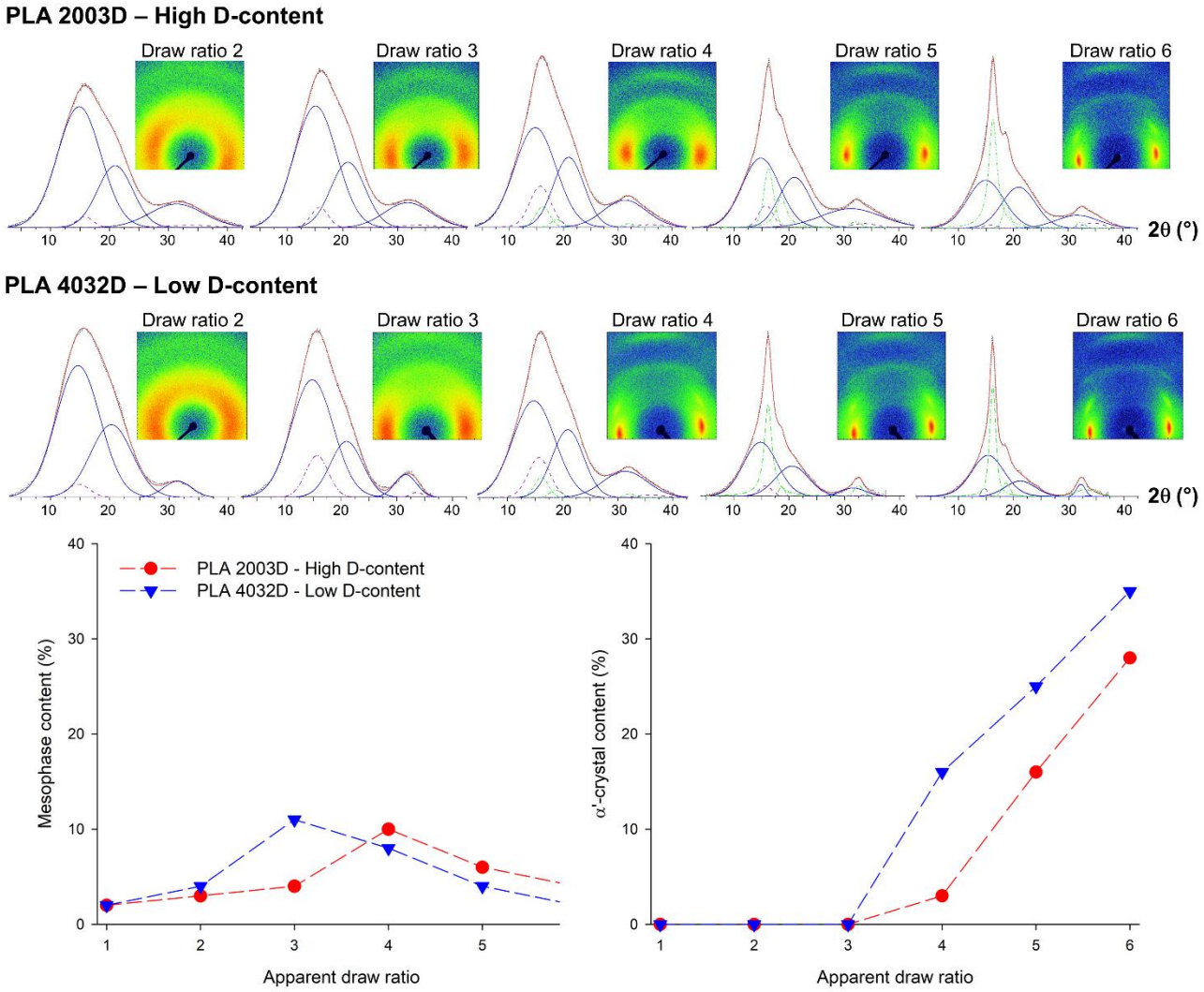

Figure 4*. 2D-WAXS spectra with corresponding WAXS intensity profiles of US-PLA films produced by extrusion – MDO at various draw ratio. Associated peak fitting with experimental profiles (red curves), fitted amorphous peaks (blue curves), fitted mesophase peaks (dotted purple curves), fitted α'-crystalline peaks (green curves). Comparative analysis between US-PLA films made from PLA 2003D and PLA 4032D in terms of phase content (mesophase and crystal phase) as a function of the draw ratio.*

WAXS analysis were also used to identify the type of strain-induced PLA crystals and quantify their amount formed during the MDO stage. For this purpose, a fitting procedure was applied to WAXS intensity profiles in order to extract the individual contribution of the amorphous phase, the mesophase and the crystalline phase. The best fits are presented in **Figure 4** for all US-PLA films. The contribution of strain-induced PLA crystals is easily extracted from WAXS intensity profiles of

US-PLA films obtained at elevated draw ratio. Actually, the contribution of the crystalline phase can be modeled by three peaks located at 16.2, 18.7 and 32.1° in agreement with (*110*)/(*200*), (*203*) and (*018*) reflection planes of the disordered α'-phase (theoretical values close to 16.4° and 18.7° for the two major peaks)[45–48,50–52]. The low number of reflection planes is also characteristic of the disordered α'-phase. The presence of the ordered α-phase is clearly excluded (theoretical values close to 16.7° and 19.1° for the two major planes) and these conclusions regarding the type of strain-induced crystals are consistent with previous thermograms of US-PLA films, in particular regarding their melting behaviors (double melting peaks and low melting temperature compared to original PLA films). The amount of disordered α'-crystals formed during MDO can be extracted using the peak fitting procedure and values are tabulated in **Table 2**. Results are highly consistent with previous results obtained by DSC. For US-PLA films made from PLA 2003D (high D-content), the strain-induced crystals appear in significative amount for draw ratio 5 and the degree of crystallinity increases up to 28 % for draw ratio 6. For US-PLA films made from PLA 4032D (low D-content), the strain-induced crystallization appears in significative amount for draw ratio 4 and a higher degree of crystallinity up to 35 % is obtained for draw ratio 6.

WAXS analysis were also used to identify the presence of a mesomorphic phase (mesophase) formed during the MDO stage, a phase currently described as a nematic-like phase with a high orientational order but poor positional/conformational order[46–48]. This mesophase is known to appear in uniaxial stretching conditions and could be quantified by WAXS. The presence of a mesophase is first suspected by DSC with the appearance of a post-T_g endotherm for several US-PLA films. For this purpose, the contribution of amorphous phase and mesophase were extracted from WAXS intensity profiles using the fitting procedure. The contribution of amorphous phase is characterized by three broad halos (located at 14.8, 21.0 and 31.4°) and the contribution of the mesophase by two shaper peaks (located at 15.7 and 33.6°)[46–48]. The presence of a mesophase is clearly attested in all US-PLA films (**Figure 4**) and the amount of mesophase is tabulated in **Table 2**. For US-PLA films made from PLA 2003D (high D-content), the amount of mesophase was found

close to 3 – 4 % at low draw ratio and increases up to 10 % for draw ratio 4. The amount of mesophase drops down for higher draw ratio. Similar observations are attested for US-PLA films made from PLA 4032 (low D-content) but the maximal amount of mesophase is found for draw ratio 3. As a conclusion, the formation of mesophase was also found more sensitive to draw ratio for US-PLA films made from PLA 4032D (low D-content) than US-PLA films made from PLA 2003D (high D-content), an effect probably attributed to the difference in terms of optical purity. The amount of mesophase remains quite low in US-PLA films, in accordance with several reports[46–48]. It can be finally mentioned that the mesophase seems to be present in small amount in extruded PLA films before the MDO stage.

US-PLA films were also submitted to FTIR analysis, a powerful technique to detect the amorphous phase, crystal phases and mesophase[43,44,50,51,60]. Actually, in the range 900 – 1000 cm^{-1}, the contribution of the amorphous phase could be clearly detected with an absorption peak centered on 956 cm^{-1}. The broad absorption peak in the range 910 – 930 cm^{-1} is linked to the mesophase (theoretical peak position 918 cm^{-1}) and to the crystal phase (theoretical peak position 923 cm^{-1}). The mesophase contribution cannot be clearly decoupled from the crystal one. A coupled contribution (mesophase + α'-crystal) can only be evaluated by FTIR and their amount is obtained through **Equation 6**. FTIR spectra of US-PLA could be found in **Figure S3**. Values of $X_{meso\text{-}crystal}$ are tabulated in **Table 2** together with the position of broad peak corresponding to the mesophase and crystal phase. Values of $X_{meso\text{-}crystals}$ are globally in accordance with WAXS and DSC results for all US-PLA films (except slight deviations at elevated draw ratio). The peak position is in agreement with the presence of mesophase at low draw ratio (without α'-crystals) and mesophase contents are consistent with WAXS results. The peak position shifts towards higher wavelengths at elevated draw ratio indicating the appearance of crystals in significative amounts. For US-PLA films made from PLA 2003D, the peak position significantly shifts at draw ratio 5. For US-PLA films made from PLA 4032D, the peak position shifts at a lower draw ratio (close to 4). All these results clearly confirm previous conclusions made by DSC and WAXS.

$$X_{meso-crystal} = \frac{A_{918-923}}{A_{918-923} + A_{956}} \quad (6)$$

with $A_{918\text{-}923}$ the area of broad absorption peak related to the mesophase/crystal phase and A_{956} the area of absorption peak related to amorphous phase

As a conclusion, the impact of the draw ratio on the amount of crystals and mesophase in US-PLA films produced by extrusion – MDO was revealed by DSC, WAXS and FTIR. For sake of clarity, results are gathered in **Figure 4**. The formation of α'-crystals appears at a critical draw ratio according to a strain-induced crystallization phenomenon. US-PLA films made from PLA 4032D display a lower critical draw ratio close to 4 (*vs*. 5 for US-PLA films made from PLA 2003D) and a higher crystallinity index close to 35 % at the maximal draw ratio (*vs*. 28 % for US-PLA films made from PLA 2003D). The mesophase is clearly observed, even at low draw ratio. The amount of mesophase first increases at low draw ratio before declining at elevated draw ratio. The same behavior is highlighted for US-PLA films made from PLA 4032D and PLA 2003D with a similar maximal amount of mesophase close to 10 %. However, the mesophase develops easier for US-PLA films made from PLA 4032D. All these results are in accordance with the optical purity of original PLA grades. Correlations could be detected between the amount of crystals / mesophase and piezoelectric properties but the orientation state of these phases (amorphous phase, mesophase and α'-crystals) also need to be investigated to draw precise conclusions.

3.3. Orientation state of US-PLA films

Along with the amount of crystals/mesophase, the orientation state of US-PLA films was thoroughly investigated and 2D-WAXS analysis were first performed. This powerful technique globally consists in recording WAXS spectra as a function of the azimuthal angle (stretching direction corresponds to a reference azimuthal angle of 0°) and the orientation state is extracted from the azimuthal distribution of a specific peak. The Herman's orientation factor *f* is then calculated from **Equation 4-5**. 2D-WAXS spectra of extruded PLA films before the MDO stage could be found in **Figure S2.** Quasi-isotropic and broad halos are obtained attesting for unoriented

and amorphous films (orientation factor *f* close to 0). 2D-WAXS spectra of US-PLA films are displayed in **Figure 4** and the presence of oriented structures are immediately attested.

For US-PLA films made from PLA 2003D (high D-content), the broad and isotropic halo turns anisotropic even at low draw in the range 2 – 3 with a maximal intensity at an azimuthal angle of 90°. The amorphous phase and the mesophase consequently are consequently oriented along the stretching direction. Sharp peaks corresponding the crystalline α'-phase are clearly detected at elevated draw ratio in the range 5 – 6. The (*110*)/(*200*) reflection plane is mainly detected at an azimuthal angle of 90° where as other (*203*) and (*018*) reflection planes are preferentially detected at azimuthal angles of 45° and 0°. Oriented crystalline phases are consequently obtained. The orientation factors *f* are tabulated in **Table S1** and monotonically increases with the draw ratio. At elevated draw ratio, the orientation factor *f* reaches 0.38 indicating a high orientation state but non-perfect along the stretching direction ($f < 1$). It can be also noticed that the apparition of α'-crystals at draw ratio 4 does not affect the evolution of the orientation factor. Similar results are obtained for US-PLA films made from PLA 4032D (low D-content), except that slightly higher orientation factors *f* are attested (maximal orientation factor *f* close to 0.41 at draw ratio 6, **Table S1**). This effect could be ascribed to higher degrees of crystallinity. 2D-WAXS analyses consequently demonstrate the production of US-PLA films with high orientation states by extrusion – MDO. Orientation states increase with draw ratio but similar orientation factors are obtained for the two PLA grades. 2D-WAXS analyses provide information about the global orientation state of US-PLA films without precise discrimination between the amorphous phase, the mesophase and the crystal phase.

In this respect, polarized FTIR analyses were conducted on US-PLA films to detect the specific orientation of these phases. Briefly, US-PLA films were twice analyzed with (i) an IR light polarized within the stretching direction (*i.e.* electric field vector parallel to the stretching direction) and (ii) an IR light polarized perpendicular to the stretching direction (*i.e.* electric field vector perpendicular to the stretching direction). In this respect, the orientation of specific chemical bonds

within the stretching direction or perpendicular to the stretching direction could be assessed. As mentioned earlier, the contribution of the amorphous phase is detected at 956 cm^{-1}. The mesophase and to the crystal phase give rise to a broad absorption peak in the range 910 – 930 cm^{-1}. For extruded PLA films before the MDO stage, the two FTIR spectra are similar attesting for un-oriented amorphous films (**Figure S4**). Typical polarized FTIR spectra of US-PLA films are displayed in **Figure 5**. For sake of clarity, polarized FTIR spectra are only presented for US-PLA films with draw ratios of 3 and 6 presented but polarized FTIR spectra for other US-PLA films could be found in **Figure S5**. An IR dichroism is clearly attested for US-PLA films and the IR dichroism increases with draw ratio. Actually, the absorption peak related to the amorphous phase is clearly more intense using an IR light polarized within the stretching direction. This effect is consistent with previous studies[43,44] and attests for a significative but non-perfect orientation of the amorphous phase along the stretching direction. A dichroic ratio $DR_{amorphous}$ can be extract from polarized FTIR spectra with the **Equation 7**. To the contrary, the absorption peak related to the mesophase and the crystal phase is clearly more intense using an IR light polarized perpendicular to the stretching direction. This effect is also consistent with previous studies[43,44] and, here, a nearly-perfect orientation of these phases within the stretching direction is deduced because absorption peaks are absent with an IR light polarized within the stretching direction. A dichroic ratio $DR_{meso-crystal}$ can be extract from polarized FTIR spectra with the **Equation 8** and values are tabulated into **Table S1**.

$$DR_{amorphous} = \frac{A^{T}_{956}}{A^{II}_{956}} \quad (7)$$

$$DR_{meso-crystal} = \frac{A^{II}_{918-923}}{A^{T}_{918-923}} \quad (8)$$

with A^{II}_{956}, $A^{II}_{918-923}$ the area of absorption peaks related to the amorphous phase and to the mesophase/crystal phase using an IR light polarized within the stretching direction and A^{T}_{956}, $A^{T}_{918-923}$ the area of absorption peaks related to the amorphous phase and to the mesophase / crystal phase using an IR light polarized perpendicular to the stretching direction

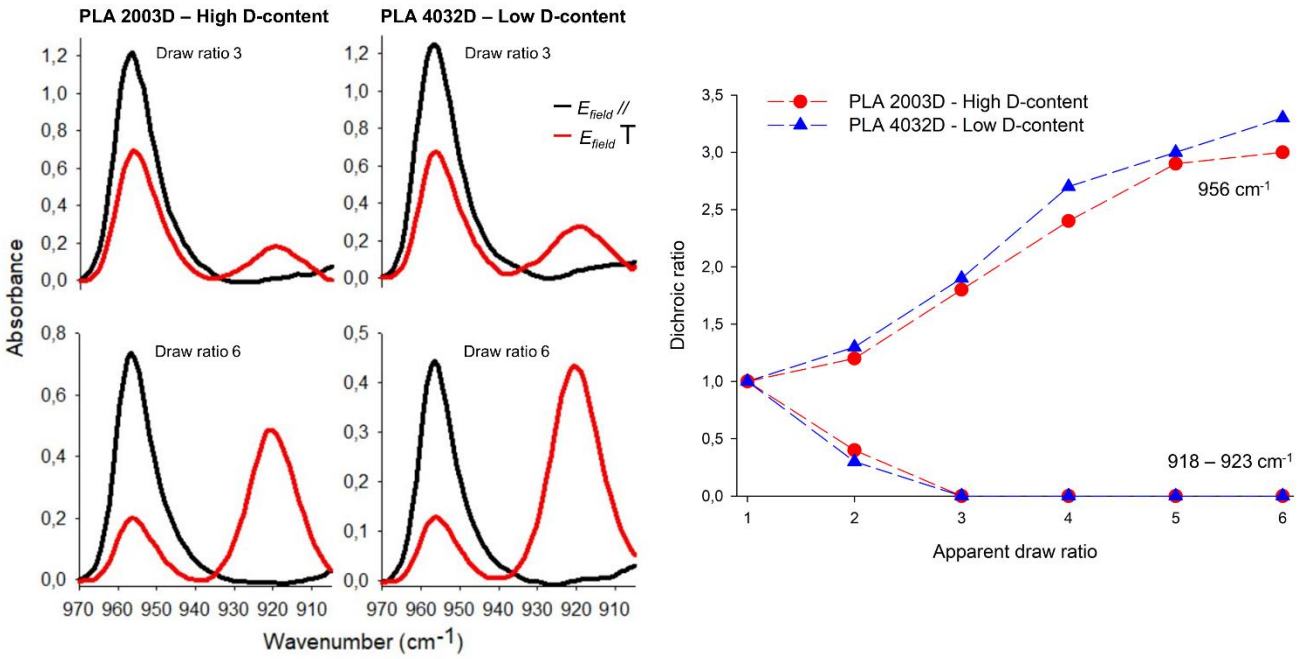

***Figure 5**. Polarized FTIR spectra of US-PLA films produced by extrusion – MDO with draw ratios of 3 and 6. FTIR spectra recorded with an IR light polarized within the stretching direction (black curves) and with an IR light polarized perpendicular to the stretching direction (red curves). Evolution of the dichroic ratios $DR_{amorphous}$ and $DR_{meso\text{-}crystal}$ with the draw ratio for US-PLA films produced by extrusion – MDO.*

Figure 5 displays the evolution of the dichroic ratios for the amorphous phase ($DR_{amorphous}$) and for the mesophase/crystal phase ($DR_{meso\text{-}crystal}$) in US-PLA films at various draw ratios. For US-PLA films made from PLA 2003D (high D-content), finite values of $DR_{amorphous}$ are obtained and $DR_{amorphous}$ increases with the draw ratio. A non-linear evolution is attested in particular at elevated draw ratios. It can be also stated out that $DR_{amorphous}$ seems to be well-below the theoretical values at any draw ratio (*i.e.* draw ratio roughly equals the dichroic ratio). A partly-oriented amorphous phase within the stretching direction is consequently produced in US-PLA films produced by extrusion – MDO. The orientation state of the amorphous phase within the stretching direction is significant and increases with the draw ratio. However, the orientation state is never perfect at any draw ratio. This classical phenomenon could arise from (i) the intrinsic orientational – relaxational dynamics of the PLA amorphous phase at the considered stretching temperature and (ii) stretching defects classically occurring during the MDO, in particular film slippage during uniaxial stretching that reduces the real draw ratio applied to the PLA films. Concerning the mesophase and the crystal

phase, a different behavior is observed. Actually, $DR_{meso\text{-}crystal}$ sharply drops to 0 for draw ratio above 2. This effect indicates that fully-oriented mesophase and crystal phase are systematically produced in US-PLA films produced by extrusion – MDO at any draw ratio. The above conclusions regarding the orientation state of the amorphous phase, mesophase and crystal phase are consistent with previous studies[43,44]. It can be finally mentioned that similar $DR_{amorphous}$ and $DR_{meso\text{-}crystal}$ values are obtained for US-PLA films made from PLA 4032D (low D-content) at any draw ratio, indicating a minor impact of the optical purity on the orientation state of US-PLA produced by extrusion – MDO.

3.4. Structure – properties relationships at low draw ratios

According to several studies, shear piezoelectric properties of PLA are proportional to the product between the degree of crystallinity (X_c) and the degree of orientation (F_c) (for moderate F_c values)[1,20–23]. This relationship is obviously quite inaccurate for as-produced US-PLA films produced by extrusion – MDO because shear piezoelectric properties are detected even for non-crystalline films. These films are composed of three phases (amorphous phase, mesophase and α'-crystal phase) with their own degree of orientation. The contribution of each phase to the overall shear piezoelectric coefficient is consequently approached. The discussion will be here limited to low draw ratios up to 4 for current US-PLA films produced by extrusion – MDO because the dramatic deterioration of the shear piezoelectric properties at elevated draw ratio cannot be explained in terms of degree of crystallinity and orientation.

The orientation states of US-PLA films made from PLA 2003D (high D-content) and PLA4032D (low D-content) are roughly similar. The differences in terms of shear piezoelectric properties are consequently solely attributed to differences in terms of mesophase and crystal contents (**Figure 6**). At draw ratio 3, the shear piezoelectric coefficient increases by 0.9 pC/N for a 7 % positive variation of the mesophase content. A significant contribution of the mesophase to the shear piezoelectric coefficient of US-PLA films is concluded with a specific shear piezoelectricity

coefficient for the fully-oriented mesophase ($d_{14\text{-mesophase}}$) extrapolated to 13 pC/N. Similarly, at draw ratio 4, the overall shear piezoelectric coefficient increases by 2.2 pC/N for a 14 % positive variation of the α'-crystal content and 2 % negative variation of the mesophase content. The classical contribution of the α'-crystal phase to the overall shear piezoelectric coefficients of US-PLA films is attested. The specific shear piezoelectric coefficient of the fully-oriented α'-crystal phase ($d_{14\text{-}\alpha'\text{-crystals}}$) is extrapolated to 18 pC/N, a value slightly higher than the one calculated for the mesophase. To fully understand the overall level of shear piezoelectricity in US-PLA films, a contribution of the partly-oriented amorphous phase must be considered. This contribution has never been envisioned in the specialized literature and a strong link to its orientation state is naturally anticipated. In this respect, a hypothetical linear relationship to draw ratio is plotted in **Figure 6**. The contribution of the partly-oriented amorphous phase is probably quite significant in US-PLA films produced by extrusion – MDO.

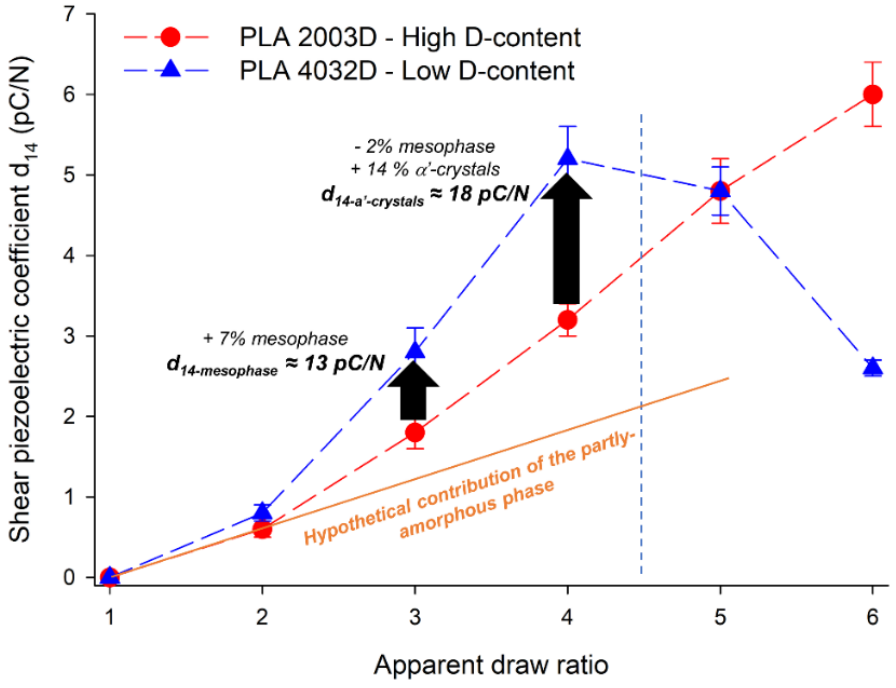

***Figure 6**. Schematic interpretations related to the contribution of the partly-oriented amorphous phase, fully-oriented mesophase and the fully-oriented α'-phase to the overall shear piezoelectric coefficient d_{14} of US-PLA films produced by extrusion – MDO.*

Based on pioneer works and current observations, a generalization is attempted and **Equation 9** is developed to link the overall shear piezoelectric coefficient d_{14} of US-PLA films with several key

structural features. These structural factors could be easily quantified and are themselves linked to MDO processing parameters.

$$d_{14} = X_a.F_a.d_{14-amorphous} + X_m.F_m.d_{14-mesophase} + X_c.F_c.d_{14-crystal} \quad (9)$$

with X_a, X_m and X_c the amount of amorphous phase, mesophase and crystal phase, F_a, F_m and F_c the orientation factor of amorphous phase, mesophase and crystal phase and $d_{14\text{-amorphous}}$, $d_{14\text{-mesophase}}$, $d_{14\text{-crystal}}$, the specific shear piezoelectric coefficient of a fully-oriented amorphous phase, a fully-oriented mesophase and a fully-oriented crystal phase.

The amount of amorphous phase, mesophase and crystal phase (X_a, X_m and X_c respectively) are easily evaluated by DSC, WAXS and FTIR. Orientation factors could be approached by 2D-WAXS and polarized FTIR. For current US-PLA films produced by extrusion – MDO, F_a depends on draw ratio but F_m and F_c are equal to 1. Specific shear piezoelectric coefficients $d_{14\text{-amorphous}}$, $d_{14\text{-mesophase}}$, $d_{14\text{-crystal}}$ represent fundamental parameters of each phase. For current US-PLA films produced by extrusion – MDO, $d_{14\text{-mesophase}}$ and $d_{14\text{-}\alpha'\text{-crystal}}$ were calculated to 13 pC/N and 18 pC/N respectively. It should be here pointed out these $d_{14\text{-mesophase}}$ and $d_{14\text{-}\alpha'\text{-crystal}}$ represents macroscopic values calculated by extrapolation to a 100 % mesophase or 100 % crystalline US-PLA films. These values are linked to the piezoelectric tensors of a single mesophase domain/crystal. Most of these nine parameters obviously depend on processing parameters (draw ratio, draw rate, draw temperature, etc) and on material parameters (molecular weight, optical purity, etc). Above values are consequently only valid for current MDO processing conditions (up to draw ratio 4) and for PLA grades used in this study. Future studies need to be conducted in order to fully validate/generalize **Equation 9** to other MDO processing conditions and to other PLA grades (or even to other oriented polymers).

3.5. Structural features controlling shear piezoelectric properties at elevated draw ratios

Shear piezoelectric properties obtained for US-PLA films produced at elevated draw ratio cannot be explained in terms of mesophase/crystal contents and orientation state. **Equation 9** is

consequently no longer valid at elevated draw ratio (*i.e.* above approx. draw ratio 4), in accordance with several studies[20–23,31,32,35]. More precisely, for US-PLA films made from PLA 4032 (low D-content), despite higher degrees of crystallinity, a dramatic deterioration of shear piezoelectric properties is detected for draw ratio higher than 5. The shear piezoelectric coefficient is even reduced by a factor 2 at the maximal draw ratio 6 and this phenomenon seems to be specific to this highly-crystalline PLA grade. Such peculiar behavior can be explained by mechanical damaging at elevated draw ratios. This hypothesis is first supported by the intense whitening of US-PLA films at draw ratio above 4 – 5 and 2D-SAXS analyses were conducted. This powerful technique globally consists in recording SAXS spectra as a function of the azimuthal angle (stretching direction corresponds to a reference azimuthal angle of 0°) and information regarding the homogeneity of US-PLA films can be extracted. 2D-SAXS spectra of extruded PLA films before the MDO stage could be found in **Figure S6**. No signal is recorded for these films that attests for highly-homogenous and isotropic amorphous films. 2D-SAXS spectra of US-PLA films are displayed in **Figure 7** with their integrated intensities (normalized by the film thickness). For US-PLA made from PLA 2003D (high D-content), no modifications of 2D-SAXS spectra are attested up to draw 3. A significative signal appears in the central region of the 2D-SAXS spectra at draw ratio 4, a signal that slightly propagates to azimuthal angles of 0° and 80/100° compared to the drawing direction. The signal strongly increases in the central region of 2D-SAXS spectra at higher draw ratios with a broad propagation centered at an azimuthal angle of 90° compared to drawing direction. Integrated SAXS profiles also display a significant increase of the normalized intensity at small scattering vectors starting from draw ratio 4. The phenomenon is amplified for draw ration 5 and 6 with a dependance of the normalized intensity to scattering vector fitting a slope -4. Heterogeneities with flat interfaces are consequently produced within US-PLA films (according to a Porod's law) and these elements are in accordance with the formation of voids / cavities aligned within the stretching direction in significative amounts at elevated draw ratios[42,61]. For US-PLA film made from PLA 4032D (low D-content), similar phenomena are observed. However, 2D-SAXS spectra indicates

that voids/cavities first appear at a lower draw ratio close to 3 with this PLA grade and, more interesting, higher normalized intensities are recorded on SAXS profiles. As a conclusion, mechanical damaging is detected for US-PLA films produced by extrusion – MDO at elevated draw ratio with the formation of void/cavities. Mechanical damaging seems to be more intense for the highly-crystalline PLA grade and a correlation is suspected with the dramatic degradation of shear piezoelectric at elevated draw ratio. It can be also finally mentioned that (i) SAXS observations are in accordance with the whitening of US-PLA films and that (ii) mechanical damaging mechanisms remain complex to determine precisely. Cavitation – crazing mechanisms starting in highly-amorphous US-PLA films coupled to the formation of shear band crazes could fit with several 2D-SAXS spectra[61] but shear yielding mechanisms cannot be totally excluded, in particular for the highly-crystalline PLA grade.

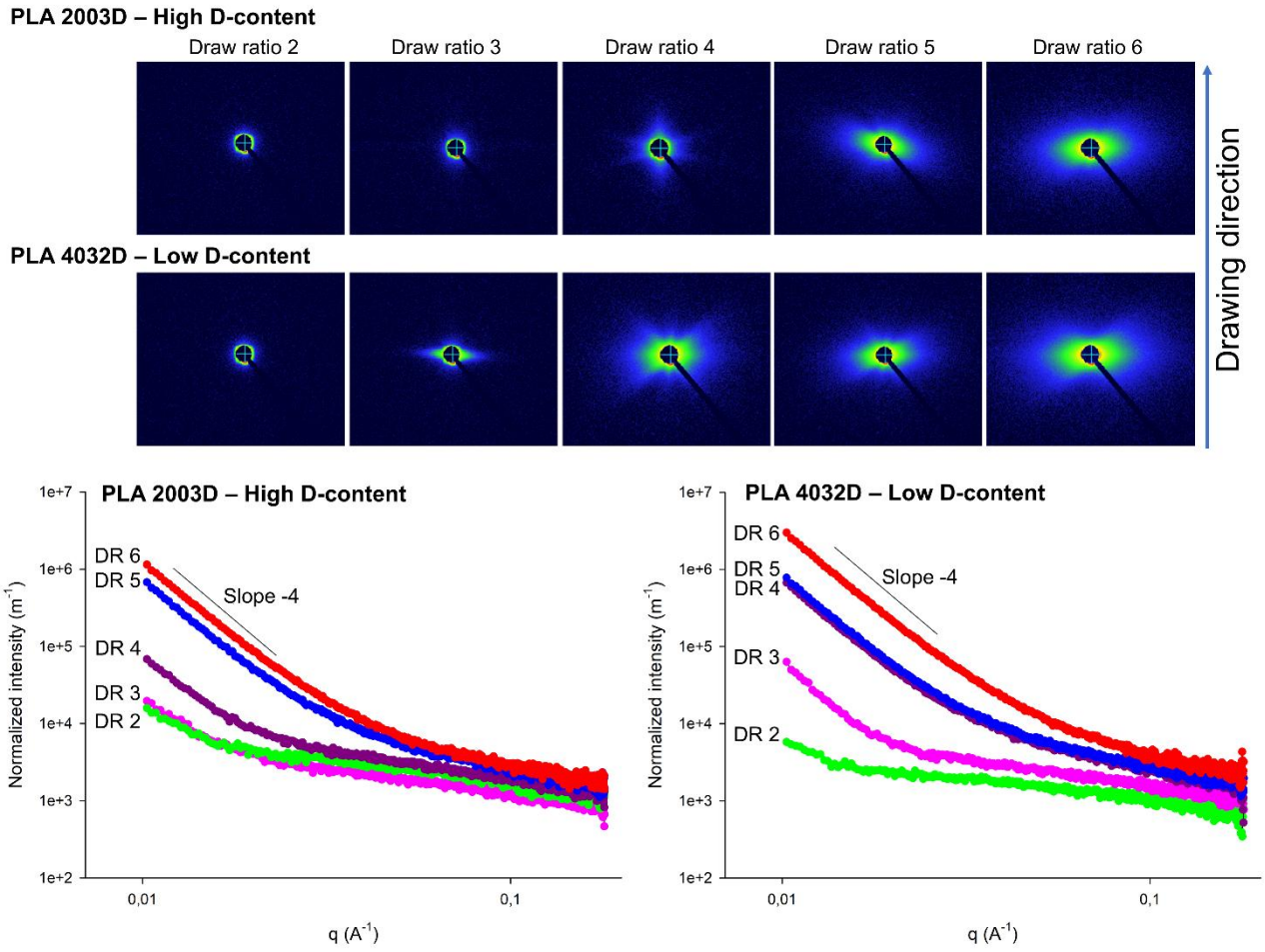

Figure 7*. 2D-SAXS spectra of US-PLA films produced by extrusion – MDO at various draw ratio (up). Experimental SAXS intensity profiles of US-PLA films produced by extrusion – MDO at various draw ratio (bottom).*

To support the correlation between void/cavity formation by mechanical damaging and the dramatic degradation of shear piezoelectric properties, complementary experiments were performed. Actually, SAXS analysis can only evaluate the amount of interface and qualitative comparison is attempted. For the normalized intensity (at a fixed scattering vector) or from the pre-exponential factor (S) of the Porod's law, the specific surface of voids/cavities produced at draw ratio 6 is higher by a factor between 1.8 – 2.6 for US-PLA films made from PLA 4032D (low D-content) (**Table S2**). However, the amount of voids/cavities cannot be obtained at these scattering factors and supplementary density – mechanical measurements were conducted. Film density (measured by a simple gravimetric – geometric method) and shear modulus (measured by dynamic mechanical analyzer) of US-PLA films are tabulated in **Table S3**. At low draw ratio (up to 3), film densities close to 1.20 g/cm^3 and shear modulus in the range 590 – 630 MPa are observed for all US-PLA films. At higher draw ratio, a significant decrease of the film density in the range 1.17 – 1.19 g/cm^3 is attested with lower shear modulus (510 – 570 MPa). However, the main phenomenon concerns US-PLA films made from PLA 4032D (low D-content) and produced at draw ratio 6. A dramatic deterioration of film density close to 1.11 g/cm3 (reduction by approx. 9 %) and of the shear modulus close to 390 MPa (reduction by approx. 35 %) is evidenced. All these elements confirmed that US-PLA films made from PLA 4032D (low D-content) is prone to intensive mechanical damaging at elevated draw ratio. Mechanically-degraded films with high void fractions are produced and, in this respect, shear piezoelectric properties of US-PLA films produced at elevated draw ratio seem to be controlled by the void fraction induced by mechanical damaging. This effect seems to be quite intense for highly-crystalline PLA grades and future investigations need to be conducted to validate the impact of voids/cavities on shear piezoelectric properties of various PLA grades (or other oriented polymers).

3.6. Discussion about the crystal structures

A final concern of high interest for final applications is related to the current maximal shear piezoelectric coefficient close to 5.9 pC/N, a value significantly lower than common shear

piezoelectric coefficients observed for oriented PLA films (close to 10 pC/N)[1,20–23]. This value is achieved at draw ratio 4 and 6 for US-PLA films made from PLA 4032D (low D-content) and from PLA 2003D (high D-content) respectively. Fully-oriented α'-crystals are obtained by extrusion – MDO based on WAXS and polarized FTIR analyses. These crystals are known to be a disordered form of the α-crystals in terms of chain conformation/packing and their presence could partly explain the gap between the current maximal shear piezoelectric coefficient and the theoretical one. However, numerous facts tend to indicate that current α'-crystals are structurally quite close the nematic liquid-crystal mesophase. First, based on FTIR analysis, the peak position of current α'-crystals is regularly observed in the range 920.1 – 920.5 cm^{-1}, even for US-PLA films with high amounts of α'-crystals and poor amounts of mesophase (**Table 2**). The peak position of current α'-crystals is located in between the theoretical value of the mesophase (918 cm^{-1}) and of the regular α'-crystals (923 cm^{-1}). More importantly, US-PLA films with a high amount of α'-crystals are marked by the absence of any peaks on SAXS intensity profiles (**Figure 7**). These peaks are potentially masked the signal of voids / cavities but it seems that current α'-crystals do not display any long-range order. In other words, current α'-crystals do not possess classical periodic and ordered stackings of lamella. These observations tend to demonstrate that current α'-crystals are structurally intermediate between the nematic liquid-crystal mesophase and classical α'-crystals obtained by thermal annealing. The structure α'-crystals produced by extrusion – MDO particularly fits with the model of condis-crystal mesophase (orientational order by 2D-WAXS/FTIR, positional order by WAXS and conformational disorder by SAXS), such a mesophase recently observed by several authors in mechanically-deformed PLA materials close to glass transition temperature[48,49]. The above conclusion explains the close values between $d_{14\text{-mesophase}}$ and $d_{14\text{-}\alpha'\text{-crystal}}$ (13 pC/N and 18 pC/N respectively), values still quite far from the value reported by Fukada E. for PLA crystals (30 pC/N) [1,20,21]. Further investigations on PLA crystal structures produced by extrusion – MDO and their specific shear piezoelectricities will be conducted in a near future.

4. Conclusions

This study is dedicated to shear piezoelectric properties of US-PLA films manufactured by an industrially-relevant extrusion – orientation process without poling and a specific insight on process – structure – properties relationships is provided. Two commercially-available PLA grades with different D-isomer contents are investigated. The shear piezoelectric coefficient d_{14} of US-PLA films increases with the draw ratio applied during the orientation stage and a maximal d_{14} of 5.9 pC/N is reported in our study. However, a dramatic degradation of piezoelectric properties is specifically observed at elevated draw ratio for PLA grades with a low D-isomer content. In this respect, relationships between draw ratio, induced structures during the orientation stage and final piezoelectric properties are investigated to improve the global knowledge on these materials and reveal potential optimization routes at the material/processing levels.

For this purpose, various characterization techniques were used such as DSC, 2D-WAXS, 2D-SAXS and polarized FTIR. The mesophase is detected up to draw ratio 3 – 4 after being replaced by a strain-induced crystallization at higher draw ratio. The two PLA grades displayed slight classical differences such as higher crystallinity and higher sensitivity to draw ratio for the PLA grade with a low D-isomer content. The amount of mesophase is quite similar between the two PLA grades. The orientation state of the amorphous phase, mesophase and α'-crystals could be assessed in our US-PLA films. A partly-oriented amorphous phase with a draw ratio-depend orientation state is attested. However, the mesophase and the α'-crystal phase are fully oriented within the orientation direction in our US-PLA films. No much differences are observed between the two PLA grades in terms of orientation state.

Shear piezoelectric properties obtained at moderate draw ratio (up to approx. 4) seem to be supported by amount and orientation of each phase. A refined model taking into account these parameters is proposed. Interestingly, the specific shear piezoelectricity of each phase was extracted from experimental data for our US-PLA films. For the first time, this fundamental parameter was obtained for the PLA mesophase ($d_{14\text{-mesophase}} \approx 13$ pC/N), a value slightly lower than the α'-crystal phase ($d_{14\text{-}\alpha'\text{-crystal}} \approx 18$ pC/N) but still quite far from the theoretical values given by Fukada E.

(approx. 30 pC/N). At higher draw ratio, the proposed model is obviously no longer valid and other structural parameters need to be considered. Mechanical damaging with the formation of voids/cavities seems to be of major importance at elevated draw ratio. Our results indicated that amount of voids/cavities could control the dramatic deterioration of shear piezoelectric performances of US-PLA films produced at high draw ratios. These phenomena are particularly critical for highly-crystalline PLA grades with low D-isomer content. It can be noticed that mechanical damaging mechanisms are still quite unclear for our US-PLA films. Another factor related to the structure of as-produced α'-crystals by extrusion – MDO is also discussed, structures that seem to be quite far from classical structures obtained by thermal annealing (in particular in terms of long-range orders). This phenomenon could limit the maximal d_{14} coefficient of US-PLA films.

This work consequently sheds light on important structural features controlling shear piezoelectric properties of US-PLA films and helps define future works on the optimization of these materials. Scientific and technological perspectives are envisioned, including (i) validation/generalization of the current model (**Equation 9**) to various MDO conditions (stretching temperature, stretching rate, pre- and post-treatments, etc.) and various PLA grades (or even other oriented polymers), (ii) in-depth investigations on mechanical damaging mechanisms with their impacts on shear piezoelectric properties (in particular for highly-crystalline PLA grades submitted to extreme draw ratio) and (iii) in-depth investigations on crystal structures/types produced during the current MDO stage with their specific shear piezoelectricities. Perspectives related to the optimization of material formulations and extrusion – MDO processing conditions are also envisioned. Applicative studies in sensing, actuation and energy harvesting are also mandatory to demonstrate the technological potential of US-PLA films. These environmental-friendly and low-cost piezoelectric films easily manufactured by a conventional process of the plastic industry are believed to compete with conventional piezoelectric materials.

Supporting Information

Supporting Information is available free of charge and includes (i) complementary analysis of extruded PLA films before the MDO stage (DSC, 2D-WAXS spectra, WAXS intensity profiles, 2D-SAXS spectra, SAXS intensity profiles, FTIR spectra and polarized FTIR spectra), (ii) complementary analysis of US-PLA films (DSC, FTIR spectra and polarized FTIR spectra), (iii) complementary quantitative data on US-PLA films (orientation function, dichroic ratios, SAXS normalized intensities, pre-exponential factor of the Porod's law, film density and shear modulus). Piezoelectric data and physico-chemical data that support the findings of this study are openly available in Zenodo at https://doi.org/10.5281/zenodo.6878598 and at https://doi.org/10.5281/zenodo.7867096 respectively.

Author Contributions

Methodology MABA – CS – SB, Investigations MABA – CS – JFT – SB – BS, Validation CS – SB – JMR, Formal analysis CS – SB – JMR, Writing and original draft preparation MABA, Writing, reviewing and editing CS – SB, Supervision CS – MFL – SB – MR – CC – JMR, Funding acquisition CS – MFL – BS – SB – CC – JMR. All authors have read and agreed to the published version of the manuscript.

Funding and Acknowledgments

All authors gratefully acknowledge Wallonia Region/Service Public de Wallonie (Belgium), West Vlaanderen Region (Belgium), Agentschap Innoveren Ondernemen (Belgium) and European Commission (FEDER) for the financial support in the framework of the INTERREG France-Wallonie-Vlaanderen program (BIOHARV project, GoToS3 portofolio). CS and MFL gratefully acknowledge both International Campus on Safety and Intermodality in Transportation (CISIT, France) and Hauts-de-France Region (France) for their contributions to funding extrusion equipments and important characterization tools (dynamic rheometers, microscopes and tensile benches). SB and JFT gratefully acknowledge both Chevreul Institute (FR 2638, France), Ministère de l'Enseignement Supérieur, de la Recherche et de l'Innovation (France), Hauts-de-France Region (France) and European Commission (FEDER) for funding X-Ray facilities.

Conflicts of Interest

The authors declare no conflict of interest. The funders had no role (i) in the design of the study, (ii) in the collection, analyses, or interpretation of data, (iii) in the writing of the manuscript and (iv) in the decision to publish the results.

References

(1) *Ferroelectric Polymers: Chemistry: Physics, and Applications*; Nalwa, H. S., Ed.; CRC Press: Boca Raton, 2014. https://doi.org/10.1201/9781482295450.
(2) Marcus, M. A. Ferroelectric Polymers and Their Applications. *Ferroelectrics* **1982**, *40* (1), 29–41. https://doi.org/10.1080/00150198208210593.
(3) Sessler, G. M. Piezoelectricity in Polyvinylidenefluoride. *J. Acoust. Soc. Am.* **1981**, *70* (6), 1596–1608. https://doi.org/10.1121/1.387225.
(4) Murayama, N.; Nakamura, K.; Obara, H.; Segawa, M. The Strong Piezoelectricity in Polyvinylidene Fluoride (PVDF). *Ultrasonics* **1976**, *14* (1), 15–24. https://doi.org/10.1016/0041-624X(76)90067-6.
(5) Martins, P.; Lopes, A. C.; Lanceros-Mendez, S. Electroactive Phases of Poly(Vinylidene Fluoride): Determination, Processing and Applications. *Prog. Polym. Sci.* **2014**, *39* (4), 683–706. https://doi.org/10.1016/j.progpolymsci.2013.07.006.
(6) Gomes, J.; Serrado Nunes, J.; Sencadas, V.; Lanceros-Mendez, S. Influence of the β-Phase Content and Degree of Crystallinity on the Piezo- and Ferroelectric Properties of Poly(Vinylidene Fluoride). *Smart Mater. Struct.* **2010**, *19* (6), 065010. https://doi.org/10.1088/0964-1726/19/6/065010.
(7) De Neef, A.; Samuel, C.; Stoclet, G.; Rguiti, M.; Courtois, C.; Dubois, P.; Soulestin, J.; Raquez, J.-M. Processing of PVDF-Based Electroactive/Ferroelectric Films: Importance of PMMA and Cooling Rate from the Melt State on the Crystallization of PVDF Beta-Crystals. *Soft Matter* **2018**, *14* (22), 4591–4602. https://doi.org/10.1039/C8SM00268A.
(8) De Neef, A.; Samuel, C.; Amorín, H.; Stoclet, G.; Jiménez, R.; Dubois, P.; Soulestin, J.; Raquez, J.-M. Beta Phase Crystallization and Ferro- and Piezoelectric Performances of Melt-Processed Poly(Vinylidene Difluoride) Blends with Poly(Methyl Methacrylate) Copolymers Containing Ionizable Moieties. *ACS Appl. Polym. Mater.* **2020**, *2* (9), 3766–3780. https://doi.org/10.1021/acsapm.0c00351.
(9) Gusarov, B.; Gusarova, E.; Viala, B.; Gimeno, L.; Cugat, O. PVDF Piezoelectric Voltage Coefficient in Situ Measurements as a Function of Applied Stress. *J. Appl. Polym. Sci.* **2016**, *133* (14), n/a-n/a. https://doi.org/10.1002/app.43248.
(10) Mishra, S.; Unnikrishnan, L.; Nayak, S. K.; Mohanty, S. Advances in Piezoelectric Polymer Composites for Energy Harvesting Applications: A Systematic Review. *Macromol. Mater. Eng.* **2019**, *304* (1), 1800463. https://doi.org/10.1002/mame.201800463.
(11) Abbasipour, M.; Khajavi, R.; Akbarzadeh, A. H. A Comprehensive Review on Piezoelectric Polymeric and Ceramic Nanogenerators. *Adv. Eng. Mater.* **2022**, *24* (6), 2101312. https://doi.org/10.1002/adem.202101312.
(12) Ramadan, K. S.; Sameoto, D.; Evoy, S. A Review of Piezoelectric Polymers as Functional Materials for Electromechanical Transducers. *Smart Mater. Struct.* **2014**, *23* (3), 033001. https://doi.org/10.1088/0964-1726/23/3/033001.
(13) Yang, Z.; Zhou, S.; Zu, J.; Inman, D. High-Performance Piezoelectric Energy Harvesters and Their Applications. *Joule* **2018**, *2* (4), 642–697. https://doi.org/10.1016/j.joule.2018.03.011.
(14) Wan, C.; Bowen, C. R. Multiscale-Structuring of Polyvinylidene Fluoride for Energy Harvesting: The Impact of Molecular-, Micro- and Macro-Structure. *J. Mater. Chem. A* **2017**, *5* (7), 3091–3128. https://doi.org/10.1039/C6TA09590A.
(15) Gao, X.; Yang, J.; Wu, J.; Xin, X.; Li, Z.; Yuan, X.; Shen, X.; Dong, S. Piezoelectric Actuators and Motors: Materials, Designs, and Applications. *Adv. Mater. Technol.* **2020**, *5* (1), 1900716. https://doi.org/10.1002/admt.201900716.
(16) Song, H.; Kim, S.; Kim, H. S.; Lee, D.; Kang, C.; Nahm, S. Piezoelectric Energy Harvesting Design Principles for Materials and Structures: Material Figure- of- Merit and Self- Resonance Tuning. *Adv. Mater.* **2020**, *32* (51), 2002208. https://doi.org/10.1002/adma.202002208.
(17) Mahapatra, S. D.; Mohapatra, P. C.; Aria, A. I.; Christie, G.; Mishra, Y. K.; Hofmann, S.; Thakur, V. K. Piezoelectric Materials for Energy Harvesting and Sensing Applications:

Roadmap for Future Smart Materials. *Adv. Sci.* **2021**, *8* (17), 2100864. https://doi.org/10.1002/advs.202100864.
(18) Jiao, P.; Egbe, K.-J. I.; Xie, Y.; Matin Nazar, A.; Alavi, A. H. Piezoelectric Sensing Techniques in Structural Health Monitoring: A State-of-the-Art Review. *Sensors* **2020**, *20* (13), 3730. https://doi.org/10.3390/s20133730.
(19) Farahani, A.; Zarei-Hanzaki, A.; Abedi, H. R.; Tayebi, L.; Mostafavi, E. Polylactic Acid Piezo-Biopolymers: Chemistry, Structural Evolution, Fabrication Methods, and Tissue Engineering Applications. *J. Funct. Biomater.* **2021**, *12* (4), 71. https://doi.org/10.3390/jfb12040071.
(20) Fukada, E. Piezoelectricity of Biopolymers. *Biorheology* **1995**, *32* (6), 593–609. https://doi.org/10.1016/0006-355X(95)00039-C.
(21) Ochiai, T.; Fukada, E. Electromechanical Properties of Poly-L-Lactic Acid. *Jpn. J. Appl. Phys.* **1998**, *37* (6R), 3374. https://doi.org/10.1143/JJAP.37.3374.
(22) Lovell, C. S.; Fitz-Gerald, J. M.; Park, C. Decoupling the Effects of Crystallinity and Orientation on the Shear Piezoelectricity of Polylactic Acid. *J. Polym. Sci. Part B Polym. Phys.* **2011**, *49* (21), 1555–1562. https://doi.org/10.1002/polb.22345.
(23) Mat Zin, S. H.; Velayutham, T. S.; Furukawa, T.; Kodama, H.; Gan, W. C.; Chio-Srichan, S.; Kriechbaum, M.; Nakajima, T. Quantitative Study on the Face Shear Piezoelectricity and Its Relaxation in Uniaxially-Drawn and Annealed Poly-l-Lactic Acid. *Polymer* **2022**, *254*, 125095. https://doi.org/10.1016/j.polymer.2022.125095.
(24) Bernard, F.; Gimeno, L.; Viala, B.; Gusarov, B.; Cugat, O. Direct Piezoelectric Coefficient Measurements of PVDF and PLLA under Controlled Strain and Stress. *Proceedings* **2017**, *1* (4), 335. https://doi.org/10.3390/proceedings1040335.
(25) Zhao, C.; Zhang, J.; Wang, Z. L.; Ren, K. A Poly(L-Lactic Acid) Polymer-Based Thermally Stable Cantilever for Vibration Energy Harvesting Applications. *Adv. Sustain. Syst.* **2017**, *1* (9), 1700068. https://doi.org/10.1002/adsu.201700068.
(26) Zhang, J.; Gong, S.; Li, X.; Liang, J.; Wang, Z. L.; Ren, K. A Wind- Driven Poly(Tetrafluoroethylene) Electret and Polylactide Polymer- Based Hybrid Nanogenerator for Self- Powered Temperature Detection System. *Adv. Sustain. Syst.* **2021**, *5* (1), 2000192. https://doi.org/10.1002/adsu.202000192.
(27) Ando, M.; Kawamura, H.; Kitada, H.; Sekimoto, Y.; Inoue, T.; Tajitsu, Y. Pressure-Sensitive Touch Panel Based on Piezoelectric Poly(L-Lactic Acid) Film. *Jpn. J. Appl. Phys.* **2013**, *52* (9S1), 09KD17. https://doi.org/10.7567/JJAP.52.09KD17.
(28) Imoto, K.; Date, M.; Fukada, E.; Tahara, K.; Kamaiyama, Y.; Yamakita, T.; Tajitsu, Y. Piezoelectric Motion of Poly(L-Lactic Acid) Film Improved by Supercritical CO2 Treatment. *Jpn. J. Appl. Phys.* **2009**, *48* (9), 09KE06. https://doi.org/10.1143/JJAP.48.09KE06.
(29) Ito, S.; Imoto, K.; Takai, K.; Kuroda, S.; Kamimura, Y.; Kataoka, T.; Kawai, N.; Date, M.; Fukada, E.; Tajitsu, Y. Sensing Using Piezoelectric Chiral Polymer Fiber. *Jpn. J. Appl. Phys.* **2012**, *51*, 09LD16. https://doi.org/10.1143/JJAP.51.09LD16.
(30) Shiomi, Y.; Onishi, K.; Nakiri, T.; Imoto, K.; Ariura, F.; Miyabo, A.; Date, M.; Fukada, E.; Tajitsu, Y. Improvement of Piezoelectricity of Poly(L-Lactide) Film by Using Acrylic Symmetric Block Copolymer as Additive. *Jpn. J. Appl. Phys.* **2013**, *52* (9S1), 09KE02. https://doi.org/10.7567/JJAP.52.09KE02.
(31) Tajitsu, Y. Development of Environmentally Friendly Piezoelectric Polymer Film Actuator Having Multilayer Structure. *Jpn. J. Appl. Phys.* **2016**, *55* (4S), 04EA07. https://doi.org/10.7567/JJAP.55.04EA07.
(32) Tajitsu, Y. Fundamental Study on Improvement of Piezoelectricity of Poly(ι-Lactic Acid) and Its Application to Film Actuators. *IEEE Trans. Ultrason. Ferroelectr. Freq. Control* **2013**, *60* (8), 1625–1629. https://doi.org/10.1109/TUFFC.2013.2744.
(33) Tajitsu, Y. Piezoelectricity of Chiral Polymeric Fiber and Its Application in Biomedical Engineering. *IEEE Trans. Ultrason. Ferroelectr. Freq. Control* **2008**, *55* (5), 1000–1008. https://doi.org/10.1109/TUFFC.2008.746.

(34) Tajitsu, Y. Sensing Complicated Motion of Human Body Using Piezoelectric Chiral Polymer Fiber. *Ferroelectrics* **2015**, *480* (1), 32–38. https://doi.org/10.1080/00150193.2015.1012410.
(35) Yoshida, M.; Onogi, T.; Onishi, K.; Inagaki, T.; Tajitsu, Y. High Piezoelectric Performance of Poly(Lactic Acid) Film Manufactured by Solid-State Extrusion. *Jpn. J. Appl. Phys.* **2014**, *53* (9S), 09PC02. https://doi.org/10.7567/JJAP.53.09PC02.
(36) Yoshida, T.; Imoto, K.; Tahara, K.; Naka, K.; Uehara, Y.; Kataoka, S.; Date, M.; Fukada, E.; Tajitsu, Y. Piezoelectricity of Poly(L-Lactic Acid) Composite Film with Stereocomplex of Poly(L-Lactide) and Poly(D-Lactide). *Jpn. J. Appl. Phys.* **2010**, *49* (9), 09MC11. https://doi.org/10.1143/JJAP.49.09MC11.
(37) Roh, Y.; Varadan, V. V.; Varadan, V. K. Characterization of All the Elastic, Dielectric, and Piezoelectric Constants of Uniaxially Oriented Poled PVDF Films. *IEEE Trans. Ultrason. Ferroelectr. Freq. Control* **2002**, *49* (6), 836–847. https://doi.org/10.1109/TUFFC.2002.1009344.
(38) Ben Achour, M. A.; Rguiti, M.; Samuel, C.; Barrau, S.; Lacrampe, M.-F.; Courtois, C. Energy Harvesting by Uniaxially-Stretched Poly(Lactide) Films at Low Tensile Strain Frequencies for Powering Wearable Sensors: Experimental Results and Theoretical Extrapolation. *Smart Mater. Struct.* **2023**, *32* (7), 075009. https://doi.org/10.1088/1361-665X/acd972.
(39) Newnham, R. E. *Properties of Materials: Anisotropy, Symmetry, Structure*; Oxford University Press: Oxford ; New York, 2005.
(40) Ben Achour, M. A.; Samuel, C.; Rguiti, M.; Barrau, S.; Courtois, C.; Lacrampe, M. Evaluation of Shear Piezoelectric Coefficients by a Bimorph Cantilever Technique for Extruded and Oriented Poly(L - lactide) Films. *Polym. Adv. Technol.* **2022**, pat.5942. https://doi.org/10.1002/pat.5942.
(41) Mulligan, J.; Cakmak, M. Nonlinear Mechanooptical Behavior of Uniaxially Stretched Poly(Lactic Acid): Dynamic Phase Behavior. *Macromolecules* **2005**, *38* (6), 2333–2344. https://doi.org/10.1021/ma048794f.
(42) Zhang, X.; Schneider, K.; Liu, G.; Chen, J.; Brüning, K.; Wang, D.; Stamm, M. Deformation-Mediated Superstructures and Cavitation of Poly (l-Lactide): In-Situ Small-Angle X-Ray Scattering Study. *Polymer* **2012**, *53* (2), 648–656. https://doi.org/10.1016/j.polymer.2011.12.002.
(43) Wang, Y.; Zhang, H.; Li, M.; Cao, W.; Liu, C.; Shen, C. Orientation and Structural Development of Semicrystalline Poly(Lactic Acid) under Uniaxial Drawing Assessed by Infrared Spectroscopy and X-Ray Diffraction. *Polym. Test.* **2015**, *41*, 163–171. https://doi.org/10.1016/j.polymertesting.2014.11.010.
(44) Hu, J.; Zhang, T.; Gu, M.; Chen, X.; Zhang, J. Spectroscopic Analysis on Cold Drawing-Induced PLLA Mesophase. *Polymer* **2012**, *53* (22), 4922–4926. https://doi.org/10.1016/j.polymer.2012.09.012.
(45) Billimoria, K.; Heeley, E. L.; Parsons, N.; Figiel, Ł. An Investigation into the Crystalline Morphology Transitions in Poly-L-Lactic Acid (PLLA) under Uniaxial Deformation in the Quasi-Solid-State Regime. *Eur. Polym. J.* **2018**, *101*, 127–139. https://doi.org/10.1016/j.eurpolymj.2018.01.031.
(46) Stoclet, G.; Seguela, R.; Lefebvre, J. M.; Elkoun, S.; Vanmansart, C. Strain-Induced Molecular Ordering in Polylactide upon Uniaxial Stretching. *Macromolecules* **2010**, *43* (3), 1488–1498. https://doi.org/10.1021/ma9024366.
(47) Stoclet, G.; Seguela, R.; Lefebvre, J.-M.; Rochas, C. New Insights on the Strain-Induced Mesophase of Poly(D , L -Lactide): *In Situ* WAXS and DSC Study of the Thermo-Mechanical Stability. *Macromolecules* **2010**, *43* (17), 7228–7237. https://doi.org/10.1021/ma101430c.
(48) Baptista, C.; Azagury, A.; Baker, C. M.; Mathiowitz, E. The Characterization and Quantification of the Induced Mesophases of Poly-l-Lactic Acid. *Polymer* **2021**, *226*, 123822. https://doi.org/10.1016/j.polymer.2021.123822.
(49) Janeczek, H.; Duale, K.; Sikorska, W.; Godzierz, M.; Kordyka, A.; Marcinkowski, A.; Hercog, A.; Musioł, M.; Kowalczuk, M.; Christova, D.; Rydz, J. Poly(L -Lactide) Liquid Crystals with

Tailor-Made Properties Toward a Specific Nematic Mesophase Texture. *ACS Sustain. Chem. Eng.* **2022**, *10* (10), 3323–3334. https://doi.org/10.1021/acssuschemeng.1c08282.
(50) Zhang, J.; Duan, Y.; Sato, H.; Tsuji, H.; Noda, I.; Yan, S.; Ozaki, Y. Crystal Modifications and Thermal Behavior of Poly(L -Lactic Acid) Revealed by Infrared Spectroscopy. *Macromolecules* **2005**, *38* (19), 8012–8021. https://doi.org/10.1021/ma051232r.
(51) Pan, P.; Zhu, B.; Kai, W.; Dong, T.; Inoue, Y. Polymorphic Transition in Disordered Poly(L -Lactide) Crystals Induced by Annealing at Elevated Temperatures. *Macromolecules* **2008**, *41* (12), 4296–4304. https://doi.org/10.1021/ma800343g.
(52) Puchalski, M.; Kwolek, S.; Szparaga, G.; Chrzanowski, M.; Krucińska, I. Investigation of the Influence of PLA Molecular Structure on the Crystalline Forms (α' and α) and Mechanical Properties of Wet Spinning Fibres. *Polymers* **2017**, *9* (12), 18. https://doi.org/10.3390/polym9010018.
(53) Hatfield, E. Machine Direction–Oriented Film Technology. In *Multilayer Flexible Packaging*; Elsevier, 2016; pp 147–152. https://doi.org/10.1016/B978-0-323-37100-1.00011-9.
(54) Drobny, J. G. Processing Methods Applicable to Thermoplastic Elastomers. In *Handbook of Thermoplastic Elastomers*; Elsevier, 2014; pp 33–173. https://doi.org/10.1016/B978-0-323-22136-8.00004-1.
(55) Standau, T.; Zhao, C.; Murillo Castellón, S.; Bonten, C.; Altstädt, V. Chemical Modification and Foam Processing of Polylactide (PLA). *Polymers* **2019**, *11* (2), 306. https://doi.org/10.3390/polym11020306.
(56) Kmetty, Á.; Litauszki, K. Development of Poly (Lactide Acid) Foams with Thermally Expandable Microspheres. *Polymers* **2020**, *12* (2), 463. https://doi.org/10.3390/polym12020463.
(57) Samuel, C.; Raquez, J.-M.; Dubois, P. PLLA/PMMA Blends: A Shear-Induced Miscibility with Tunable Morphologies and Properties? *Polymer* **2013**, *54* (15), 3931–3939. https://doi.org/10.1016/j.polymer.2013.05.021.
(58) Samuel, C.; Cayuela, J.; Barakat, I.; Müller, A. J.; Raquez, J.-M.; Dubois, P. Stereocomplexation of Polylactide Enhanced by Poly(Methyl Methacrylate): Improved Processability and Thermomechanical Properties of Stereocomplexable Polylactide-Based Materials. *ACS Appl. Mater. Interfaces* **2013**, *5* (22), 11797–11807. https://doi.org/10.1021/am403443m.
(59) Samuel, C.; Barrau, S.; Lefebvre, J.-M.; Raquez, J.-M.; Dubois, P. Designing Multiple-Shape Memory Polymers with Miscible Polymer Blends: Evidence and Origins of a Triple-Shape Memory Effect for Miscible PLLA/PMMA Blends. *Macromolecules* **2014**, *47* (19), 6791–6803. https://doi.org/10.1021/ma500846x.
(60) Meaurio, E.; López-Rodríguez, N.; Sarasua, J. R. Infrared Spectrum of Poly(L -Lactide): Application to Crystallinity Studies. *Macromolecules* **2006**, *39* (26), 9291–9301. https://doi.org/10.1021/ma061890r.
(61) Stoclet, G.; Lefebvre, J. M.; Séguéla, R.; Vanmansart, C. In-Situ SAXS Study of the Plastic Deformation Behavior of Polylactide upon Cold-Drawing. *Polymer* **2014**, *55* (7), 1817–1828. https://doi.org/10.1016/j.polymer.2014.02.010.

Table of Contents Graphic

Oriented PLA films by MDO

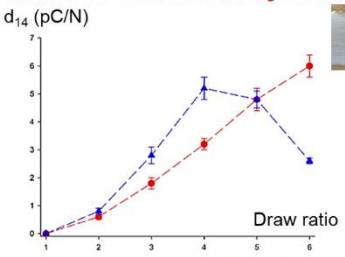

Shear piezoelectricity

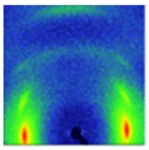

Structural analysis